Supporting Information

An Intelligent, Autocatalytic, DNAzyme Biocircuit for Amplified Imaging of Intracellular MicroRNA

Meirong Cui, Dan Zhang, Qingfu Wang, Jie Chao*

Key Laboratory for Organic Electronics and Information Displays, Jiangsu Key Laboratory for Biosensors, Institute of Advanced Materials (IAM), Jiangsu National Synergetic Innovation Center for Advanced Materials (SICAM), Nanjing University of Posts and Telecommunications, Nanjing 210023, P. R. China

*Corresponding author: Jie Chao Email：iamjchao@njupt.edu.cn. (J. Chao)

Table of contents

Reagents. Manganese chloride tetrahydrate ($MnCl_2$•$4H_2O$) was purchased from Aladdin (Shanghai, China). Tetrachloroauric acid (III) hydrate ($HAuCl_4$•$3H_2O$), trisodium citrate (NaCit), 3-(4,5-dimethylthiazol-2-yl)-2,5-diphenyl bromide Azole (MTT) and SH-PEG were purchased from Sigma-Aldrich Inc. (St. Louis, MO). Hoechst 33342 and Lysotracker™ Green DND-26 were purchased from Invitrogen (Shanghai, China). High glucose DMEM and 1640 medium were purchased from KGI (Nanjing, China), and fetal bovine serum (FBS) was from Gibco Life Technologies. All other reagents were of analytical grade and were used without purification. Ultrapure water (resistivity 18.2 MΩ cm at 25 °C) from a Millipore purification system was used throughout the experiment.

Apparatus. Zeta potential and DLS were tested with a Malvern instrument (Nano-Z, Malvern Instruments Ltd., UK). UV-vis absorption spectras were recorded on a UV-vis spectrophotometer (UV-3600, Shimadzu Co., Japan). Transmission electron micrographs were acquired on a JEM-2100 transmission electron microscope (JEOL Ltd., Japan). Fluorescence emission spectra were acquired on a Shimadzu Fluorescence S-3 spectrophotometer (RF-5301PC, Shimadzu Co., Japan). Confocal fluorescence images of cells were obtained with an Olympus FV3000 confocal fluorescence microscope (Leica, Germany). Cell viability assays were performed using Thermo Scientific Varioskan Flash (Thermo Fisher Scientific, USA).

Table S1 Sequences of oligonucleotides used for the miR-21 detection in this work.

Name	Sequence (5'-3')
H1	TTTTTTCAACATCAGTCTGATAAGCTACCATGTGT AGATAGCTTATCAGAC(Alexa-Fluor635) GCGCGAAATAGTG
H2	ATCTCTTCTCCGAGCCGGTCGCAGTCTGATAAGTC ACTACACATGGTAGCTTATCAGACTGATGCCATG TCTAGA
S	TAGCTTATCAGACTGATGTTGACACTA/ra/GGAAG AGATGGCTATTCGGCACACAAGTGG
L	CCACTTGTGCCGAATAGCCTAAAAGATAAAGTCA GATATGCTA
miR-21	UAGCUUAUCAGACUGAUGUUGA
mis-miR-21	CACAGCCGGACTACTCCTAGTG
Random DNA	AAGCTTATCTGACTGATGTTGT
miR-141	UAACACUGUCUGGUAAAGAUGG
miR-182	UUUGGCAAUGGUAGAACUCACACU
miR-197	UUCACCACCUUCUCCACCCAGC

Table S2 Sequences of oligonucleotides used for the miR-155 detection in this work.

Name	Sequence (5'-3')
155-H1	TTTTTACCCCTATCACGATTAGCATTAACCATGTGTAGATTAATGCTAAT(Alexa-Fluor635) CGCGAAATAGTGACCCC
155-H2	ATCTCTTCTCCGAGCCGGTCGATTAGCATTAATCTACACATGGTTAATGCTAATCGTGATAGGCCATGTGTAGA
155-S	TTAATGCTAATCGTGATAGGGGTCACTAT/ra/GGAAGAGATGGCTATTCGGCACACAAGTGG
155-L	CCACTTGTGCCGAATAGCCTAAAAGATAAACGATAAGCATTAA
miR-155	UUAAUGCUAAUCGUGAUAGGGGU

Supplemental Figures

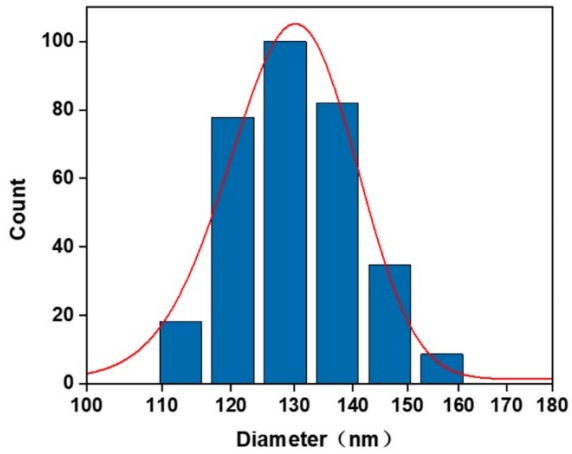

Fig. S1 The DLS measurements of the MnO_2 nanosheets after sonication for 24 h.

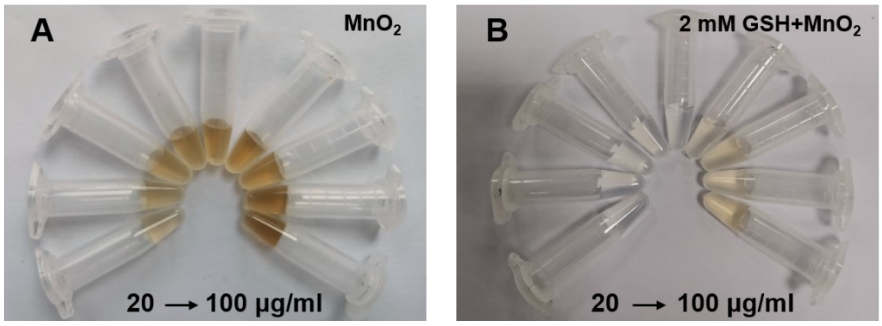

Fig. S2 Photograph of MnO_2 nanosheets (20 to 100 μg/mL) solution before (A) and after (B) adding 2.0 mM GSH.

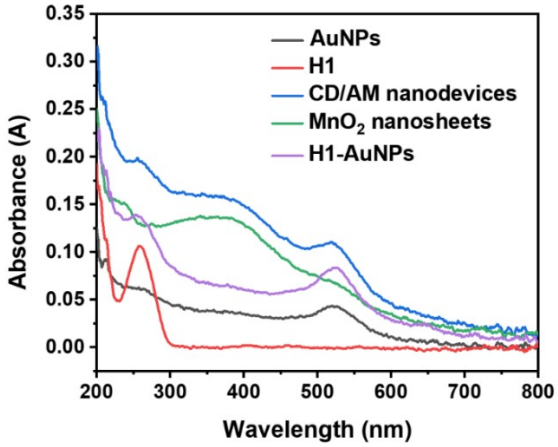

Fig. S3 The UV-vis spectrum of AuNPs, H1, CD/AM nanodevices, MnO_2 nanosheets and H1-AuNPs.

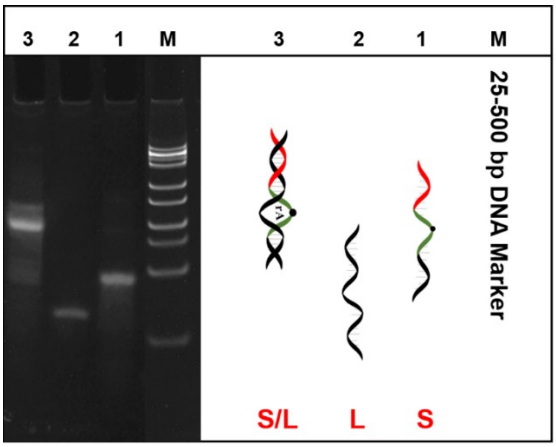

Fig. S4 Gel electrophoresis characterization of the successful formation of dsDNA "S/L". From right to left, M: 25-500 bp DNA marker; lane 1: ssDNA "S" (1μM); lane 2: ssDNA "L" (1μM); lane 3: dsDNA "S/L" (1μM).

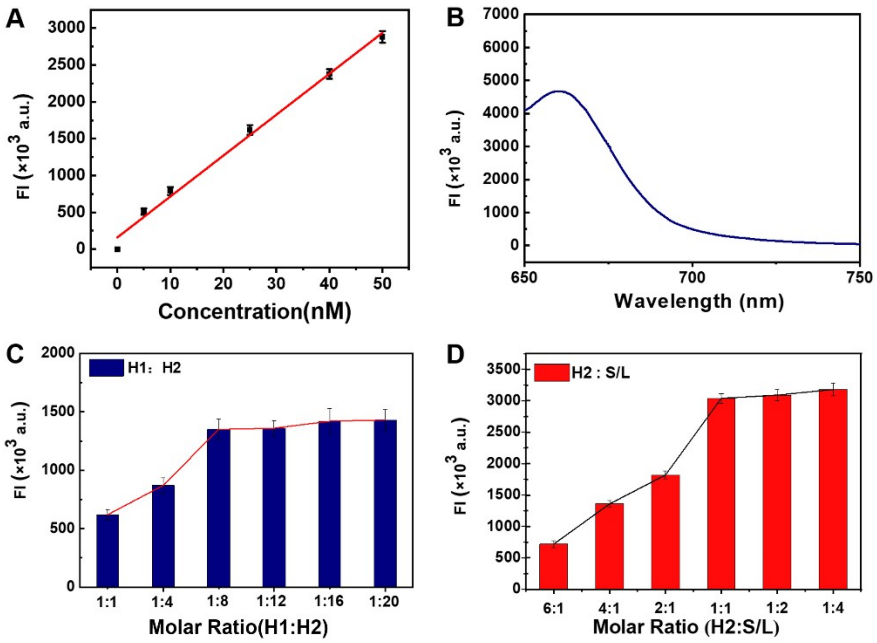

Fig. S5 Fluorescence-based method to calculate the number of DNA loading on single AuNP and DNA-AuNPs on the MnO_2 nanosheets. (A) Standard curve for the fluorescence intensity of H1 with different concentrations. (B) Fluorescence spectrum of a representative mercaptoethanol treated functionalized AuNP sample (AuNP concentration was 1 nM). The amount of H1 was calculated to be 81 molecules per AuNP. (C) and (D) Fluorescence response of the CD/AM nanodevice with different molar ratio (H1:H2 and H2:S/L) for target miR-21 detection in the presence of GSH.

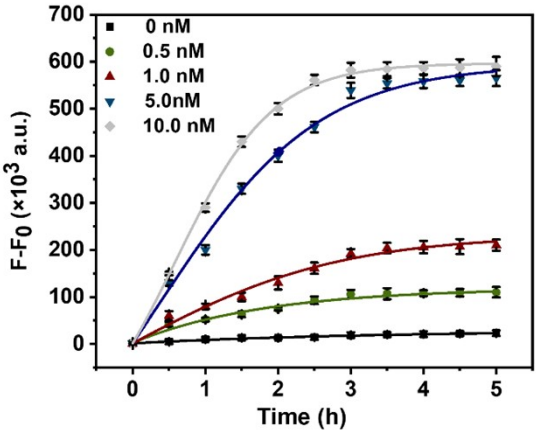

Fig. S6 Time-dependent fluorescence changes of the cross-catalytic circuit at different concentrations of target miR-21: 10.0, 5.0, 1.0, 0.5 and 0 nM.

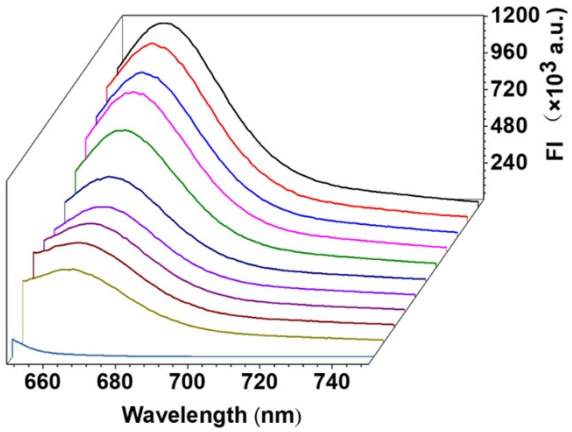

Fig. S7 Fluorescence spectra of the CD/AM nanodevice in response to different concentrations of miR-21 (0, 0.05, 0.1, 0.5, 1, 1.5, 3, 5, 10, 20, 50, 100 nM) in vitro at 37 °C, excited at 635 nm.

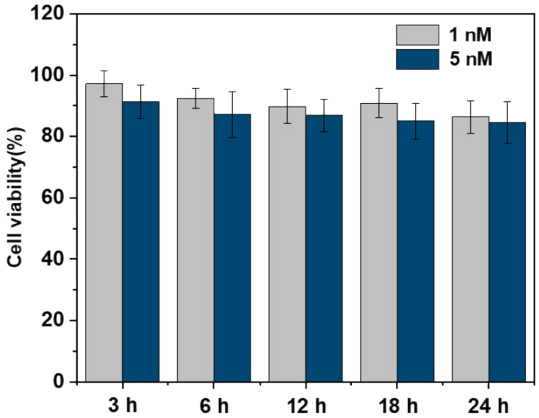

Fig. S8 Cell viability of MCF-7 cells incubated with 1 nM CD/AM nanodevice and 5 nM CD/AM

nanodevice. Error bars represent the standard deviation of five replicates.

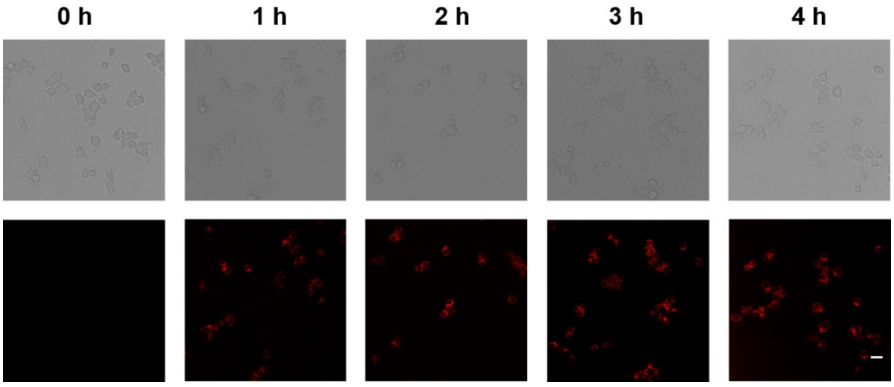

Fig. S9 Time-dependent CLSM images of MCF-7 cells incubated with CD/AM nanodevice. Emission was collected by red channel (Cy5) at 660-750 nm with 635 nm excitation, scale bars: 20 μm.

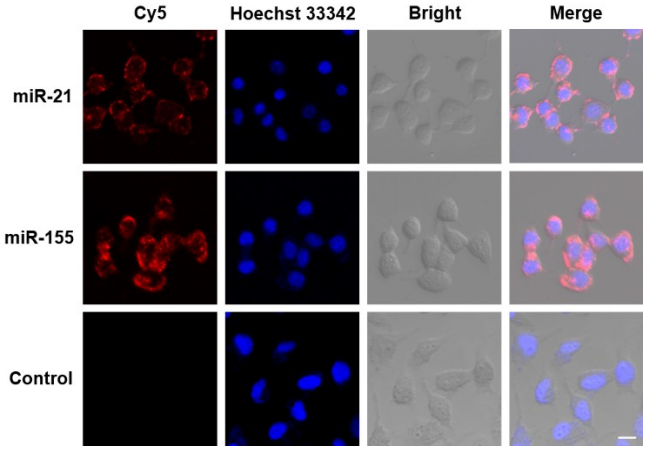

Fig. S10 CLSM images of MCF-7 cells incubated with CD/AM nanodevice, CD/AM nanodevice 155, and PBS. Emission was collected by red channel (Cy5) at 660-750 nm with 635 nm excitation, scale bars: 20 μm.